EXPLOSIBILITY OF NONTRADITIONAL DUSTS: EXPERIMENTAL AND MODELING CHALLENGES

Paul Amyotte[a,*], Faisal Khan[b], Simon Boilard[a], Ivan Iarossi[a,c], Chris Cloney[a,d], Ashok Dastidar[e], Rolf Eckhoff[f], Luca Marmo[c] and Robert Ripley[d]
[a]Process Engineering & Applied Science, Dalhousie University, Halifax, NS, Canada
[b]Process Engineering, Memorial University, St. John's, NL, Canada
[c]Dipartimento di Scienza Applicata e Tecnologia, Politecnico di Torino, Torino, Italia
[d]Martec, Lloyd's Register, Halifax, NS, Canada
[e]Fauske & Associates, Burr Ridge, IL, USA
[f]Physics and Technology, University of Bergen, Bergen, Norway
*Corresponding Author: 902–494–3976; paul.amyotte@dal.ca

The current paper describes experimental and modeling research for a series of nontraditional particulate fuel/air systems: nanomaterials, flocculent materials and hybrid mixtures. At the time of writing, experimentation is at the following stages: (i) nanomaterials – completed with data analysis performed, (ii) flocculent materials – completed with data analysis performed, and (iii) hybrid mixtures – underway (about 70 % completed) with data analysis in the early stages. Modeling work is also underway and includes phenomenological, thermokinetic and computational fluid dynamics (CFD) considerations.

KEYWORDS: Dust explosions, nanomaterials, flocculent material, hybrid mixtures

INTRODUCTION

Dust explosion risk reduction has been the subject of intensive research in the public and private sectors for several decades. This research has led to many advances including improved understanding of dust explosion fundamentals (Eckhoff, 2003), enhanced mitigation techniques such as venting and suppression (Barton, 2002), and recognition of the role of inherently safer design in dust explosion prevention and mitigation (Kletz and Amyotte, 2010).

There remains, however, a strong need for continued research on dust explosions – especially for dusts that may be termed nontraditional when compared with the more common and often-tested micron-size, spherical particles comprising a single-fuel powder; Worsfold et al. (2012) may be consulted for an overview on this point. The current paper describes the results obtained, and work in progress, from a comprehensive research program aimed at investigating the hazards and ensuing risk of the following nontraditional particulate fuel systems: (i) nanomaterials having particles with approximate dimensions between 1 and 100 nm (Boilard et al., 2012), (ii) flocculent (fibrous) materials characterized by a length-to-diameter ratio rather than a particle diameter (Iarossi et al., 2012), and (iii) hybrid mixtures consisting of a combustible dust and a flammable gas (or a combustible dust pre-wetted with a flammable solvent).

The specific fuel/air systems being studied in the above nontraditional categories are as follows: (i) micron- and nano-size titanium powder, (ii) flocculent polyamide 6.6 and polyester materials, and (iii) lactose and microcrystalline cellulose dusts admixed with methanol, ethanol and isopropanol solvents. Relevant industrial applications are the handling of metallic nano-powders, fabric and textile processing, and pharmaceutical manufacturing, respectively.

METHODOLOGY

The research undertaken is aimed at characterizing the above fuel/air systems from both experimental and modeling perspectives. Explosibility parameters investigated include maximum explosion pressure (P_{max}), size-normalized maximum rate of pressure rise (K_{St}), minimum explosible concentration (MEC), minimum ignition energy (MIE), and minimum ignition temperature (MIT). ASTM (American Society for Testing and Materials) protocols (ASTM, 2011a-d) are being followed using standard dust explosibility test equipment (Siwek 20-L explosion chamber, MIKE 3 ignition energy apparatus, and BAM oven for ignition temperature measurement).

Apparatus and procedural descriptions can be found on the equipment manufacturer's web site (http://www.kuhner.com/). In addition, a schematic diagram of the Siwek 20-L chamber setup is shown in Figure 1. This apparatus is used to determine P_{max}, K_{St} and MEC.

NANOMATERIALS

Explosibility data for the micron- and nano-size titanium samples are shown in Table 1. Here, 'ND' means 'Not Determined'. MIE results are reported as a range of values both with and without an inductance of 1mH; where applicable, E_s (the 'statistic energy' determined by manufacturer (Kuhner)-supplied software based on probabilistic considerations) is also given.

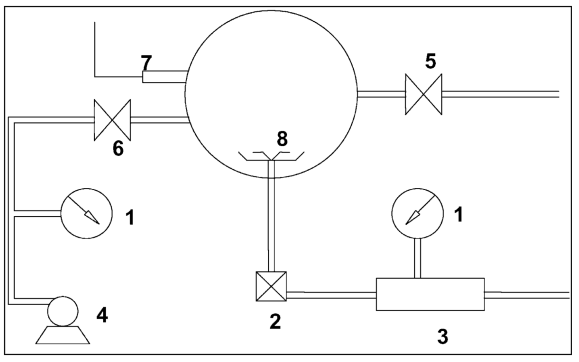

Figure 1. Schematic diagram of Siwek 20-L chamber (1 – Pressure Gauge; 2 – Solenoid Valve; 3 – Dust Storage Container; 4 – Vacuum Pump; 5 – Exhaust Valve; 6 – Vacuum Valve; 7 – Transducers; 8 – Rebound Nozzle).

The minimum ignition temperature (MIT) data in Table 1 illustrate that nano-size titanium is ignitable by relatively low hot-surface temperatures (much lower than the micron-size samples). Both micron- and nano-size titanium are ignitable by low spark energies as shown by the MIE data in Table 1.

The enhanced spark ignitability of the nano-titanium is illustrated by Figures 2(a) and 2(b) which compare MIKE 3 ignition graphs for the −325 mesh (<45 μm) and 150 nm samples, respectively. (In Figures 2(a) and 2(b), dust amount appears on the x-axis and spark energy on the y-axis; the open boxes indicate no ignition at the particular delay time and the solid boxes indicate ignition.) The nano-size sample is clearly ignitable at lower spark energies and significantly lower dust amounts (concentrations) than the micron-size sample.

Table 1 also gives Siwek 20-L data (P_{max}, $(dP/dt)_{max}$, K_{St} and MEC) for the micron-size titanium samples and, to a lesser extent, for the nano-size samples. The micron-size data show the expected increase in P_{max} and K_{St} with decreasing particle size to a limit that may be imposed by particle agglomeration effects.

The nano-titanium samples proved to be highly reactive – so much so that they could not be dispersed in air from the dust storage container (item 3 in Figure 1) into the actual 20-L chamber without exploding due to ignition by static/frictional sparking. (An exception is the tests leading to the MEC values given in Table 1, wherein the lowest dust concentrations used permitted testing with nitrogen as the dispersion gas; see the ensuing discussion in the next paragraphs.) Figure 3(a) shows a routine 20-L pressure/time trace for one of the micron-size samples; one can see the pressure rise due to dust dispersion into the 20-L chamber followed by the ignitors firing and then the dust itself exploding. Figure 3(b) shows a pressure/time trace for the finest nano-size sample (40–60 nm) with dust dispersion via the typical procedure. Here one sees an overlap of the dust dispersion and explosion steps, with the ignitors firing after the dust has exploded. (The pressure values in Figure 3(b) must be interpreted in light of the fact that the pressure transducers used are piezoelectric and hence measure only dynamic pressure changes, not static values.)

The implication of the above observations is that nano-size titanium cannot be dispersed into the 20-L chamber with air as the carrier gas. The use of nitrogen for this purpose has been previously shown to be effective by Wu et al. (2010), and further investigation in this regard was undertaken in our work as shown by Table 2.

Table 2 illustrates that no suitable combination of experimental conditions could be identified so as to disperse the nano-size titanium into the 20-L chamber and achieve a pressure/time trace of the type shown in Figure 3(a). Numerous attempts were made by varying: (i) dust concentration, (ii) dispersion gas (nitrogen or air), (iii) dispersion gas pressure and ignition delay time (both of which affect dust cloud turbulence intensity), (iv) location of the dust prior to dispersion (placed in either the external dust storage container or the 20-L chamber itself), and (v) expected oxygen concentration in the 20-L chamber once dispersion was complete. Although no external ignition source (i.e., chemical ignitors) was used in these tests, the result was an explosion similar to that shown in Figure 3(b) in every case.

Table 1. Deflagration parameters for micron- and nano-size titanium.

Size	P_{max} [bar(g)]	$(dP/dt)_{max}$ [bar/s]	K_{St}* [bar · m/s]	MEC [g/m^3]	MIE [mJ]		MIT [°C]
					Ind. (E_s)	No Ind. (E_s)	
−100 mesh (<150 μm)	5.5	84	23	60	10–30 (23)	1–3 (1.7)	>590
−325 mesh (<45 μm)	7.7	436	118	60	1–3 (1.7)	1–3 (2.3)	460
≤20 μm	6.9	420	114	50	<1	<1	460
150 nm	ND	ND	ND	40	ND	<1	250
60–80 nm	ND	ND	ND	50	ND	<1	240
40–60 nm	ND	ND	ND	50	ND	<1	250

*K_{St}, the previously mentioned size-normalized maximum rate of pressure rise, is the product of the maximum rate of pressure rise, $(dP/dt)_{max}$, and the cube-root of the volume, V, of the chamber in which the explosion tests were conducted. The units of K_{St} are therefore units of (pressure)(length)/(time); conventional units are bar · m/s. In the tests reported here, the explosion chamber volume is 20 L or 0.02 m^3.

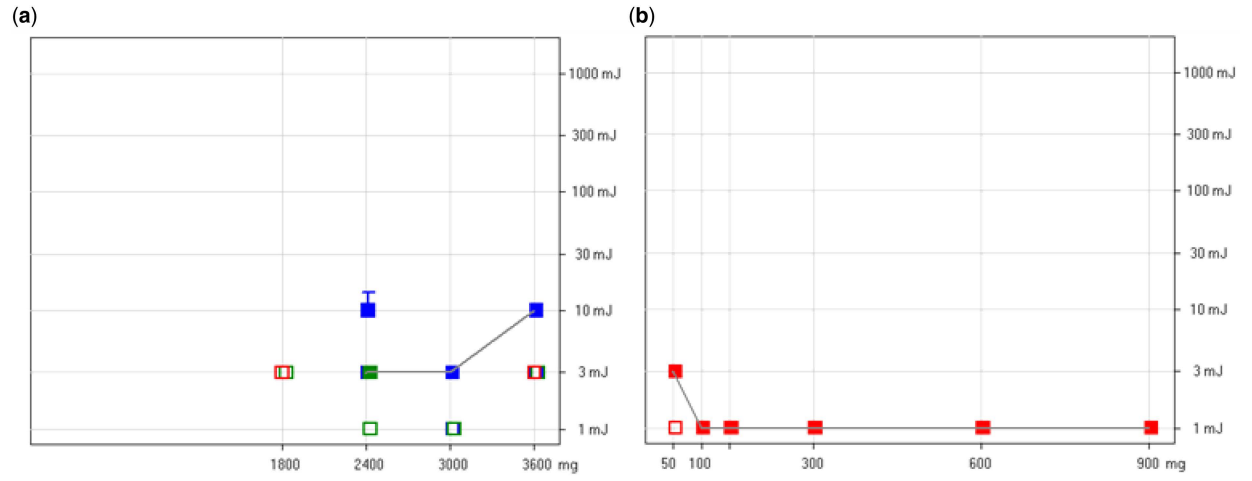

Figure 2. (a) Minimum ignition energy data (no inductance) for −325 mesh (<45 μm) titanium. (b) Minimum ignition energy data (no inductance) for 150 nm titanium.

As previously mentioned, the only exception to this occurrence was the MEC testing for the nano-titanium samples (Table 1). Here, dispersion with nitrogen at dust concentrations of the order of 50 g/m^3 and lower enabled the formation of a dust cloud in the 20-L chamber and ignition (or non-ignition) by an external source (5-kJ ignitor in the case of MEC testing). Because the explosion chamber must be partially evacuated prior to dust dispersion in all tests, the use of nitrogen as the carrier gas required first backfilling the chamber with pure oxygen to the desired partial pressure. This ensured that the oxygen concentration in the 20-L chamber was 21% at the time of ignitor firing. The entire procedure of nitrogen dispersion into an environment having an initially elevated oxygen concentration was verified by testing with a dust for which explosion data were available for the normal air dispersion procedure.

Because of the high nano-titanium reactivity, the decision was made to also conduct inerting tests with nano-size titanium dioxide (10–30 nm). The TiO_2 itself was first tested in the 20-L chamber and determined, as expected, to be chemically inert. Tests were then carried out with increasing percentages of TiO_2 admixed with the 150 nm titanium (at a constant Ti concentration of 125 g/m^3). Nitrogen was used as the dispersion gas with the final oxygen concentration in the explosion chamber arranged to be 21%.

For admixed TiO_2 amounts up to 60% of the total dust mass, pre-ignitions of the type shown in Figure 3(b)

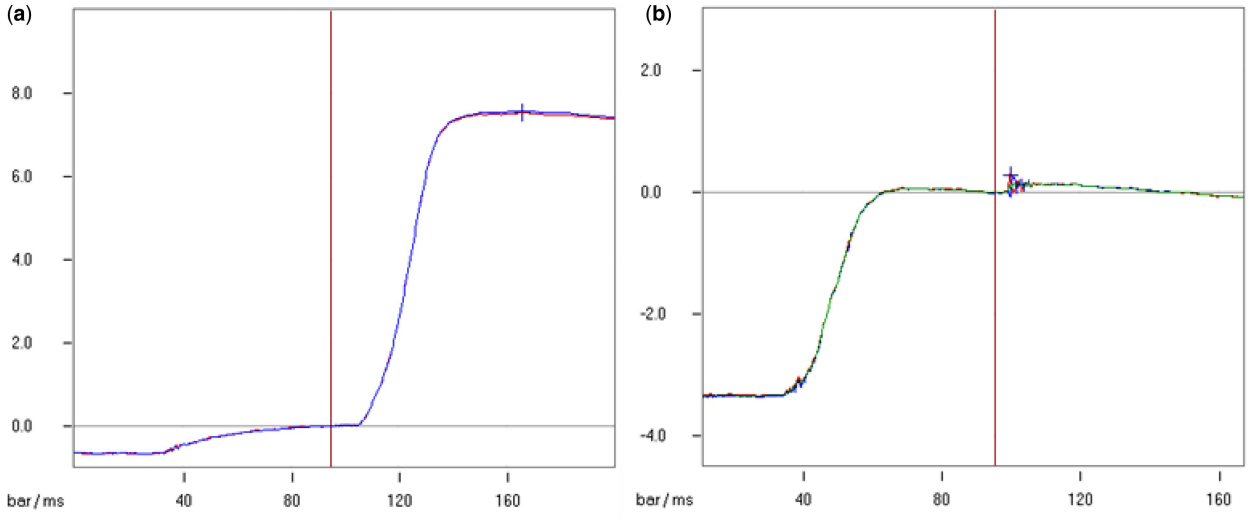

Figure 3. (a) Pressure/time trace (Siwek 20-L chamber) for −325 mesh (<45 μm) titanium at 1750 g/m^3. (b) Pressure/time trace (Siwek 20-L chamber) for 40–60 nm titanium at 100 g/m^3.

Table 2. Trials with various experimental conditions for 150 nm titanium (no chemical ignitors).

Dust Concentration [g/m^3]	Dispersion Gas	Dispersion Pressure [bar(g)]	Ignition Delay Time [ms]	Dust Placement (Figure 1)	Final O_2 % in 20-L Chamber	Explosion During Dispersion?
125	N_2	20	60	In Item 3	21	YES
125	N_2	20	60	In Item 3	19.5	YES
125	N_2	20	60	In Item 3	17.6	YES
125	N_2	20	60	In Item 3	15	YES
125	N_2	20	60	In Item 3	9	YES
500	Air	20	60	Under Item 8	21	YES
500	Air	20	60	On Item 8	21	YES
500	Air	10	60	On Item 8	21	YES
500	Air	10	120	On Item 8	21	YES
500	Air	5	120	On Item 8	21	YES
500	N_2	20	60	On Item 8	9	YES
250	N_2	10	60	On Item 8	9	YES

were observed for the mixture. At 80% TiO_2 pre-ignition did not occur, meaning that the dust was successfully dispersed into the explosion chamber; ignition of the resulting dust cloud was then achieved by means of a 5-kJ ignitor. A concentration of 85% TiO_2 rendered the mixture inert from the perspectives of both pre-ignition during dispersion and ignition by a 5-kJ external energy source. It is interesting to note that these findings are in general accordance with the large body of knowledge on coal dust inerting with the admixture of rock dust (limestone, dolomite, etc.) This suggests that the TiO_2 acts as a thermal inhibitor in the same manner as rock dust.

To conclude this section, mention is made of the following precautions taken during experimentation with the nano-size titanium:

- Proper PPE (personal protective equipment) was worn at all times. This included a filtered mask, safety glasses, face shield (when working with chemical ignitors), lab coat and nitrile gloves.
- Adequate ventilation was ensured both in the lab and for the exhaust from the 20-L chamber.
- The lab was assessed for concentrations of airborne nanoparticles using two different particle counters: FLUKE model 983 for particles in the range of 300 nm to 10 μm, and KANOMAX handheld CPC model 3800 for particles in the range of 15 nm to 1 μm.
- The nano-titanium packages supplied by the manufacturer were opened and handled in a glove bag filled with nitrogen to avoid (to the greatest extent possible) contact of the titanium with oxygen and moisture in the air.

FLOCCULENT MATERIALS

Explosibility data for the tested polyamide 6.6 and polyester samples are shown in Tables 3 and 4. (The explanations given in the first paragraph of the previous section on nanomaterials apply here as well.) The parameter dtex (or decitex) is a unit of measure for the linear density of fibers and is equivalent to the mass in grams per 10,000 meters. It can be thought of as a measure of fiber diameter.

Because of the low bulk density of the flocculent samples, a test procedure was developed for the 20-L chamber in which a maximum of 15 g of dust were placed in the external dust storage container (item 3 in Figure 1). This corresponds to a dust concentration of 750 g/m^3; for higher concentrations, the remainder of the sample amount was placed directly in the 20-L chamber around the rebound nozzle (item 8 in Figure 1).

Table 3. Deflagration parameters for polyamide 6.6 with changing length.

dtex	Length [mm]	P_{max} [bar(g)]	$(dP/dt)_{max}$ [bar/s]	K_{St} [bar · m/s]	MEC [g/m^3]	MIE [mJ]		MIT [°C]
						Ind. (E_s)	No Ind.	
3.3	0.3	7.1	178	48	75	300–1000 (580)	>1000	475
3.3	0.5	6.6	135	37	125	>1000	ND	485
3.3	0.75	6.4	102	28	155	>1000	ND	485
3.3	0.9	6.3	102	28	160	>1000	ND	485
3.3	1.0	6.4	94	26	165	>1000	ND	490

Table 4. Deflagration parameters for polyamide 6.6 and polyester with changing diameter.

Material	dtex	Length [mm]	P_{max} [bar(g)]	$(dP/dt)_{max}$ [bar/s]	K_{St} [bar · m/s]	MEC [g/m^3]	MIE [mJ] Ind. (E_s)	MIE [mJ] No Ind.	MIT [°C]
Polyamide 6.6	1.7	0.5	6.6	183	50	50	300–1000 (540)	>1000	485
Polyamide 6.6	3.3	0.5	6.6	135	37	125	>1000	ND	485
Polyester	1.7	0.5	6.9	247	67	70	300–1000 (330)	>1000	495
Polyester	3.3	0.5	5.5	104	28	70	300–1000 (390)	>1000	495

Considering the fibers as cylinders, the specific surface area (surface area per unit volume) at constant diameter is inversely proportional to fiber length. Thus, an increase in length results in a decrease in specific surface area and hence a decrease in P_{max} and K_{St}, and an increase in MEC (Table 3).

Similarly, at constant length the specific surface area is inversely proportional to fiber diameter. As shown in Table 4, increasing the diameter (dtex) has a significant effect on P_{max} and K_{St} due to the corresponding decrease in specific surface area – much more so for the polyester than the polyamide 6.6 sample. The difference between the behaviour of the two polymers likely results from their different chemical structures. The presence of phenyl groups in the polyester structure may be key to understanding the greater influence of dtex on P_{max} and K_{St} for this material than for the polyamide 6.6. Moreover, the structure of polyester could lead to a reduced tendency to coagulate and produce a sort of polymeric network – the formation of which would be expected to affect dispersion and increase the MIE. The data in Table 4 support this concept; the MIE for polyester is seen to undergo a far less significant change than for polyamide 6.6 with an increase in dtex.

Further support for the arguments in the previous paragraph is given by Figures 4 and 5, which show scanning electron micrographs (SEMs) of polyamide 6.6 before and after explosion, respectively. Post-explosion, polyamide 6.6 displays an expansive network due to melting, with the cylindrical fibers becoming shorter and thicker. The fibers also have a greater tendency to coagulate and form spherical aggregates – again, hindering dispersion and leading to an increase in MIE (Marmo and Cavallero, 2008).

Table 4 illustrates that the two materials tested have different hazard profiles when the data are considered in terms of likelihood of explosion occurrence (MEC, MIE and MIT) and severity of explosion consequences (P_{max} and K_{St}). In Table 3, the data suggest a characteristic upper length for polyamide 6.6 beyond which the explosibility parameters do not change significantly (e.g., P_{max} and K_{St} do not appreciably decrease).

As a final note on flocculent dust combustion, Figure 6 demonstrates that these dusts are readily flammable and can present the additional hazard of being an ignition source for other materials present in flock-handling facilities. In the top photograph of Figure 6 showing primary flame propagation, flame is generally visible only from the electrode position upward through the glass tube. Secondary flame propagation occurs in the bottom photograph of Figure 6 after the initial upward flow reverses and dust at the bottom of the tube is ignited. Afterward, a sticky,

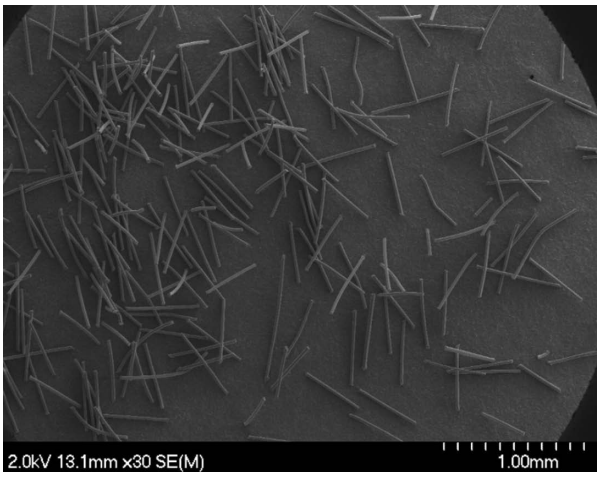

Figure 4. Scanning electron micrograph of polyamide 6.6 (3.3 dtex and 0.5 mm length) pre-explosion.

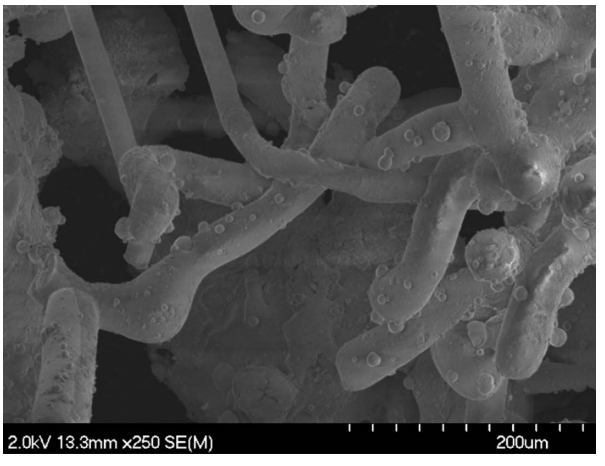

Figure 5. Scanning electron micrograph of polyamide 6.6 (3.3 dtex and 0.5 mm length) post-explosion.

interwoven residue structure was found coating the interior of the glass tube.

HYBRID MIXTURES

Hybrid mixture research is typically conducted with three possible approaches: (i) gaseous solvent at room temperature existing in the combustion atmosphere prior to dust dispersal, (ii) liquid solvent at room temperature requiring flashing-off for admixture to the combustion atmosphere prior to dust dispersal, and (iii) liquid solvent at room temperature admixed as a liquid with the dust prior to dust dispersal.

The research underway in the current project utilizes the latter two of the above approaches with common pharmaceutical excipients and solvents. These are the previously mentioned lactose and microcrystalline cellulose (MCC), and methanol, ethanol and isopropanol, respectively. All materials tested are pharmaceutical-grade in terms of composition and, in the case of the solids, particle size distribution. Because the MIKE 3 apparatus and BAM oven are not closed systems, only baseline excipient (dust)-alone testing and excipient pre-wetted with solvent testing are possible for MIE and MIT determination in our laboratory. With the Siwek 20-L chamber (i.e., a closed system), however, it is feasible to conduct P_{max}, K_{St} and MEC testing for all three cases of the dust alone, pre-wetted with solvent, and with solvent admixed to the combustion atmosphere prior to dust dispersal.

At the time of writing, P_{max}, K_{St}, MEC, MIE and MIT tests have been conducted (with ongoing data analysis) for lactose and MCC, and also for each dust pre-wetted with methanol, ethanol and isopropanol at 80% of the lower flammability limit for each solvent. Testing remains to be done for P_{max}, K_{St} and MEC of the dusts with solvent admixed directly to the combustion atmosphere. We anticipate that our hybrid mixture testing and data analysis will be completed over the ensuing months before Hazards XXIII. A full reporting of materials, methodologies, results and conclusions will be the subject of future correspondence from the current authors.

As preliminary commentary, we offer the following thoughts on data trends and experimental challenges. In all cases, pre-wetting of MCC and lactose with solvent had a measurable impact on each explosibility parameter (P_{max}, K_{St}, MEC, MIE and MIT). As expected, the influence

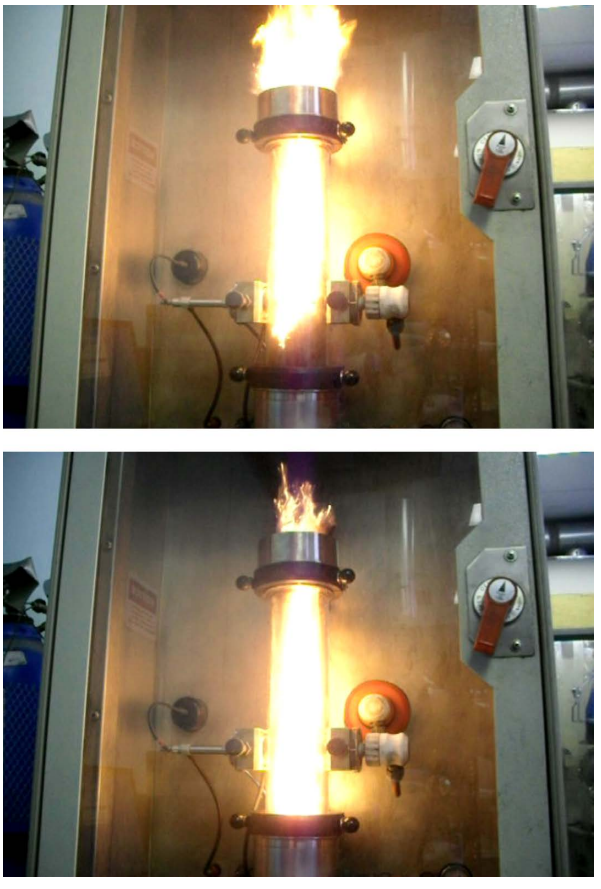

Figure 6. Top: Primary flame propagation of polyamide 6.6 (1.7 dtex and 0.5 mm length) in MIKE 3 apparatus (1200 mg dust and 120 ms ignition delay time). Bottom: Secondary flame propagation of polyamide 6.6 (1.7 dtex and 0.5 mm length) in MIKE 3 apparatus (1200 mg dust and 120 ms ignition delay time).

was generally an enhancement of the particular parameter (e.g., increase in K_{St}, decrease in MIE, etc.); the lone exception was P_{max} for MCC which displayed a decrease of 0.6–0.8 bar(g) with solvent admixture. Additionally, while the magnitude of the effect of solvent admixture to MCC was generally distinguishable for the different solvents, this was not the case for lactose. Pre-wetting of lactose with each of the three solvents resulted in similar values of P_{max}, K_{St} and MIE.

Key experimental challenges encountered to-date include: (i) development of a consistent procedural approach to pre-wetting the excipient with solvent so as to ensure uniform coverage, and (ii) conducting MEC testing with dust and admixed solvent. In the latter case, only limited experimentation could be done because of the small amounts of dust involved in MEC testing and the resulting solubility issues. Thus, while the influence of admixed solvent on excipient MEC was clearly observed, actual MEC values for the hybrid mixtures could not be determined.

MODELING

Modeling efforts are currently underway with the following approaches and challenges:

- High-level phenomenological modeling using previously generated flocculent material explosibility data and four geometric equivalence models: radial equivalence, volumetric equivalence, surface area equivalence, and specific surface area equivalence (Amyotte et al., 2012). Here, the surface area equivalence model was determined to provide the best estimate of rate of pressure rise when compared to the limited experimental data available.
- Thermokinetic modeling of the flocculent experimental data reported in the current paper in a manner similar to previous work with spherical polyethylene data (Di Benedetto et al., 2010). This work involves consideration of a flocculent dust equivalent diameter in the development of a more sophisticated approach to account for the essentially two-dimensional nature of flocculent dust. Again, surface area equivalence considerations were employed to model the fibers as cylinders and to determine an equivalent spherical diameter. Model predictions for rate of pressure rise of polyamide 6.6 were in good agreement with the corresponding experimental data in Tables 3 and 4 (Russo et al., 2012). The use of thermokinetic modeling in this manner demonstrated the transition from a regime of pyrolysis chemical kinetic control to one of external heat transfer control with increasing equivalent diameter (i.e., increasing fiber length).
- Correlation of hybrid mixture explosibility data on the basis of the burning velocity of the admixed solvents, as previously demonstrated for polyethylene and various hydrocarbons (Amyotte et al., 2010). As per the previous discussion of hybrid mixture experimentation, it appears that burning velocity considerations alone may adequately account for the enhanced K_{St} values brought about by solvent pre-wetting of microcrystalline cellulose (with laminar burning velocities of 56 cm/s for methanol, 42 cm/s for ethanol and 41 cm/s for isopropanol). This does not appear, however, to be the case for solvent pre-wetting of lactose, which resulted in similar K_{St} values for each lactose/solvent hybrid mixture. Consideration of physical properties such as solvent latent heat of vaporization, and excipient heat capacity and solubility, may be required to attempt a phenomenological explanation of the observed data trends. It is anticipated that further insight will be provided by the upcoming experiments with solvent admixture by flashing-off into the partially evacuated 20-L chamber prior to dust dispersal.
- Computational fluid dynamics (CFD) modeling of ignitor preconditioning during dust explosion testing using the *Chinook* explosion and gas dynamics code (Cloney et al., 2012). This work has demonstrated that use of an energetic ignition source (e.g., 10 kJ) in a 20-L chamber can result in spatial and temporal variations in fluid temperature and pressure, and particle temperature and concentration, which may not be present in a larger 1-m^3 test chamber. The implications for dust explosibility testing and modeling require further consideration that is being undertaken by the current authors.
- CFD modeling of industrial-scale scenarios using the GexCon software *DESC* (Dust Explosion Simulation Code), consistent with our previous work in this area (Abuswer et al., 2011). There are several challenges here: (i) Nanomaterials – DESC is not designed to model explosions of metal dusts. Limited experimental data on carbon nanotubes are available in the literature and these data may offer a modeling alternative to nano-titanium (although not a direct comparison to our experimental data reported here). (ii) Flocculent materials – Sufficient details on flock-processing equipment geometry and size have not yet been found in the literature. We have, however, recently used DESC to successfully predict explosion pressures for polyamide 6.6 and polyester in 20-L and 1-m^3 spheres. (iii) Hybrid mixtures – DESC is not designed to model the ignition sequence for hybrid mixtures, which is a feature of interest in industry given that hybrid mixtures can ignite even when both components (solid and gaseous) exist in concentrations below their respective minimum explosible concentration and lower flammability limit. Nevertheless, it is still possible to employ DESC for overpressure prediction of hybrid mixture explosions by means of appropriate input data for the mixture explosibility characteristics and thermodynamic properties.

The phenomenological and thermokinetic modeling will help to better understand the hazardous nature of the nontraditional fuel/air systems so as to facilitate implementation of prevention and mitigation measures. The CFD modeling is aimed largely at consequence assessment to be combined with probabilistic fault tree analysis in a quantitative risk management framework for dust and hybrid mixture explosions.

CONCLUDING REMARKS

Experimental data have been provided in this paper for micron- and nano-size titantium, and flocculent polyamide 6.6 and polyester. A companion set of data for hybrid mixtures typically found in the pharmaceutical industry has also been partially developed. Phenomenological, thermokinetic and CFD modeling approaches have been described in terms of their role in quantitatively assessing and managing explosion hazards arising from nontraditional dusts. Unique challenges exist with respect to gaps in the knowledge base for these materials; the overall problem of dust explosions is far from being solved.

ACKNOWLEDGEMENT

The authors gratefully acknowledge the financial assistance of the Natural Sciences and Engineering Research Council (NSERC) of Canada in the form of a strategic grant.

REFERENCES

Abuswer, M., Amyotte, P. and Khan, F., 2011, A quantitative risk management framework for dust and hybrid mixture explosions, *Journal of Loss Prevention in the Process Industries*, doi:10.1016/j.jlp.2011.08.010.

Amyotte, P., Lindsay, M., Domaratzki, R., Marchand, N., Di Benedetto, A. and Russo, P., 2010, Prevention and mitigation of dust and hybrid mixture explosions, *Process Safety Progress*, 29: 17–21.

Amyotte, P.R., Cloney, C.T., Khan, F.I. and Ripley, R.C., 2012, Dust explosion risk moderation for flocculent dusts, *Journal of Loss Prevention in the Process Industries*, in press (accepted May 19, 2012).

ASTM, 2011a, *ASTM E1226-10 – Standard test method for explosibility of dust clouds*, American Society for Testing and Materials: West Conshohocken, PA.

ASTM, 2011b, *ASTM E1515-07 – Standard test method for minimum explosible concentration of combustible dusts*, American Society for Testing and Materials: West Conshohocken, PA.

ASTM, 2011c, *ASTM E1491-06 – Standard test method for minimum autoignition temperature of dust clouds*, American Society for Testing and Materials: West Conshohocken, PA.

ASTM, 2011d, *ASTM E2019-03 – Standard test method for minimum ignition energy of a dust cloud in air*, American Society for Testing and Materials: West Conshohocken, PA.

Barton, J. (editor), 2002, *Dust explosion prevention and protection. A practical guide*, Institution of Chemical Engineers: Rugby, UK.

Boilard, S.P., Amyotte, P.R., Khan, F.I., Dastidar, A.G. and Eckhoff, R.K., 2012, Explosibility of micron- and nano-size titanium powders, *Paper No. 009, Proceedings of 9th International Symposium on Hazards, Prevention, and Mitigation of Industrial Explosions*, Krakow, Poland (July 23–27, 2012).

Cloney, C.T., Amyotte, P.R., Khan, F.I. and Ripley, R.C., 2012, Quantifying the effect of strong ignition sources on particle preconditioning and distribution in the 20-L chamber, *Paper No. 013, Proceedings of 9th International Symposium on Hazards, Prevention, and Mitigation of Industrial Explosions*, Krakow, Poland (July 23–27, 2012).

Di Benedetto, A., Russo, P., Amyotte, P. and Marchand, N., 2010, Modelling the effect of particle size on dust explosions, *Chemical Engineering Science*, 65: 772–779.

Eckhoff, R.K., 2003, *Dust explosions in the process industries*, 3rd edition, Gulf Professional Publishing/Elsevier: Boston, MA.

Iarossi, I., Amyotte, P.R., Khan, F.I., Marmo, L., Dastidar, A.G. and Eckhoff, R.K., 2012, Explosibility of polyamide and polyester fibers, *Paper No. 004, Proceedings of 9th International Symposium on Hazards, Prevention, and Mitigation of Industrial Explosions*, Krakow, Poland (July 23–27, 2012).

Kletz, T. and Amyotte, P., 2010, *Process plants. A handbook for inherently safer design*, 2nd edition, CRC Press/Taylor & Francis Group: Boca Raton, FL.

Marmo, L. and Cavallero, D., 2008, Minimum ignition energy of nylon fibres, *Journal of Loss Prevention in the Process Industries*, 17: 449–465.

Russo, P., Amyotte, P.R., Khan, F.I. and Di Benedetto, A., 2012, Modeling of the effect of size on flocculent dust explosions, *Paper No. 054, Proceedings of 9th International Symposium on Hazards, Prevention, and Mitigation of Industrial Explosions*, Krakow, Poland (July 23–27, 2012).

Worsfold, S.M., Amyotte, P.R., Khan, F.I., Dastidar, A.G. and Eckhoff, R.K., 2012, Review of the explosibility of nontraditional dusts, *Industrial & Engineering Chemistry Research*, 51: 7651–7655.

Wu, H.-C., Kuo, Y.-C., Wang, Y.-H., Wu, C.-W. and Hsiao, H.-C., 2010, Study on safe air transporting velocity of nanograde aluminum, iron, and titanium, *Journal of Loss Prevention in the Process Industries*, 23: 308–311.